Rate Constants for a Mechanism Including Intermediates in the Interconversion of Ternary Complexes by Horse Liver Alcohol Dehydrogenase†

V. Chandra Sekhar and Bryce V. Plapp*
Department of Biochemistry, The University of Iowa, Iowa City, Iowa 52242
Received July 14, 1989; Revised Manuscript Received January 3, 1990

ABSTRACT: Transient kinetic data for partial reactions of alcohol dehydrogenase and simulations of progress curves have led to estimates of rate constants for the following mechanism, at pH 8.0 and 25 °C:

$$E \rightleftharpoons E\text{-}NAD^+ \rightleftharpoons {}^*E\text{-}NAD^+ \rightleftharpoons E\text{-}NAD^+\text{-}RCH_2OH \rightleftharpoons E\text{-}NAD^+\text{-}RCH_2O^- \rightleftharpoons {}^*E\text{-}NADH\text{-}RCHO \rightleftharpoons E\text{-}NADH\text{-}RCHO \rightleftharpoons E\text{-}NADH \rightleftharpoons E$$

Previous results show that the E–NAD^+ complex isomerizes with a forward rate constant of 620 s^{-1} [Sekhar, V. C., & Plapp, B. V. (1988) *Biochemistry 27*, 5082–5088]. The enzyme–NAD^+–alcohol complex has a pK value of 7.2 and loses a proton rapidly (>1000 s^{-1}). The transient oxidation of ethanol is 2-fold faster in D_2O, and proton inventory results suggest that the transition state has a charge of −0.3 on the substrate oxygen. Rate constants for hydride ion transfer in the forward or reverse reactions were similar for short-chain aliphatic substrates (400–600 s^{-1}). A small deuterium isotope effect for transient oxidation of longer chain alcohols is apparently due to the isomerization of the E–NAD^+ complex. The transient reduction of aliphatic aldehydes showed no primary deuterium isotope effect; thus, an isomerization of the E–NADH–aldehyde complex is postulated, as isomerization of the E–NADH complex was too fast to be detected. The estimated microscopic rate constants show that the observed transient reactions are controlled by multiple steps.

The mechanism of horse liver alcohol dehydrogenase (EC 1.1.1.1) has been extensively investigated, but rate constants for each step in a complete mechanism have not been determined under one set of conditions, and the kinetic significance of intermediates in the transient reactions has not been fully evaluated (Pettersson, 1987). The three-dimensional structures of the apoenzyme and its complexes with coenzyme and substrates show that the enzyme changes conformation upon binding coenzyme (Eklund & Brändén, 1987; Colonna-Cesari et al., 1986); the rate of this conformational change could limit the transient rate of oxidation of alcohol (Sekhar & Plapp, 1988). A proton is released from the enzyme-bound alcohol with an apparent rate constant of 250 s^{-1} at pH 7.6 (Morris et al., 1980; Shore et al., 1974), but this reaction could be controlled by isomerization of the enzyme–NAD^+ complex. Spectral evidence for an intermediate, such as E^1–NAD^+–RCH_2O^-, in the oxidation of *p*-nitrobenzyl alcohol was obtained with enzyme that had cobalt substituted for the active site zinc (Koerber et al., 1983; Sartorius et al., 1987), but the rate constants for formation and oxidation of such alkoxides have not been estimated. The availability of computer programs for kinetic simulations (Barshop et al., 1983; Zimmerle et al., 1987) now make it possible to combine data from various partial reactions and to describe the mechanism more completely.

Experimental Procedures

Reagent-grade chemicals were used as received unless specified otherwise. Phenol red was obtained from Fisher Scientific, and chlorophenol red and thymol blue were from Nutritional Biochemicals. Pyrazole, 2,2,2-trifluoroethanol (Gold Label), and deuterium oxide (99.8% pure) were from Aldrich. Acetaldehyde (MCB/Aldrich), propanal (Eastman), butanal, benzaldehyde, hexanal, benzyl alcohol, 1-propanol, and 1-butanol (Fisher) were distilled prior to use. Ethanol-d_6, 1-propanol-*1,1*-d_2, 1-butanol-d_9, and benzyl alcohol-α,α-d_2 were from Merck Sharp and Dohme Isotopes. LiNAD^+ and Na_2NADH were grade I reagents from Boehringer-Mannheim. Solutions of coenzymes and substrates were prepared just before performing kinetic studies. Concentrations of coenzymes were determined with ϵ_{260} = 18 mM^{-1} cm^{-1} for NAD^+ and ϵ_{340} = 6.22 mM^{-1} cm^{-1} for NADH. Crystalline horse liver alcohol dehydrogenase (Boehringer-Mannheim) was dissolved in a high ionic strength buffer and freed of ethanol by gel filtration on a column of Sephadex G-50 equilibrated with the appropriate buffer. For routine experiments, 33 mM sodium phosphate buffer, pH 8, was used, but 1 mM buffer was used when enzyme was prepared for pH dependence or proton release experiments. The concentration of active sites of enzyme was determined by titration (ϵ_{300} = 7.2 mM^{-1} cm^{-1}) with NAD^+ and pyrazole (Theorell & Yonetani, 1963). NADD[1] was prepared as described by Ganzhorn and Plapp (1988), except that a linear gradient of 5–250 mM sodium phosphate buffer, pH 8, was used to develop the DEAE-Sepharose column.

A Kinetic Instruments stopped-flow spectrophotometer with a path length of 2.0 cm and a dead time of about 1.3 ms and On-Line Instruments Systems software were used to obtain transient data and the observed rate constants. All reactions were studied at 25 °C in 33 mM sodium phosphate buffer, pH 8, unless stated otherwise. In general, enzyme (20 μN, 0.8 mg/mL) in one syringe was mixed with an equal volume of coenzyme and substrate and/or other ligand from the other syringe. Concentrations given in tables and figures represent the final concentrations in the reaction mixtures. The change in absorbance (ϵ = 5.5 mM^{-1} cm^{-1}) at 328 nm, which is the

†This work was supported by Grant AA00279 from the National Institute on Alcohol Abuse and Alcoholism, U.S. Public Health Service.
* Address correspondence to this author at the Department of Biochemistry, 4-370 Bowen Science Building, The University of Iowa, Iowa City, IA 52242.

[1] Abbreviations: E, horse liver alcohol dehydrogenase; NADD, (4*R*)-[4-^{2}H]nicotinamide adenine dinucleotide.

0006-2960/90/0429-4289$02.50/0

Table I: Kinetic Constants for the Transient Oxidation of Primary Alcohols[a]

alcohol	concn (mM)	K_m (mM)	k_{max} (s^{-1})	^Dk	k/K_m (mM^{-1} s^{-1})
ethanol	1.0–50	4.1	180	3.8	44
ethanol-d_5	1.0–50	2.3	48		21
propanol	0.1–5.0	1.3	310	1.5	240
propanol-1,1-d_2	0.1–5.0	0.78	205		260
butanol	0.1–7.5	0.51	310	1.3	610
butanol-d_9	0.1–5.0	0.53	240		440
hexanol	0.05–4.0	0.13	320		2400
benzyl alcohol	0.01–1.5	0.03	24	3.6	780
benzyl alcohol-α,α-d_2	0.01–1.5	0.08	6.5		83

[a] The formation of NADH from reactions of about 10 μN enzyme with 2 mM NAD^+ and varied concentrations of alcohols, producing an increase in absorbance at 328 nm, was fitted by an equation for a first-order reaction followed by a zero-order steady state. The first-order rate constants increased hyperbolically as the concentration of alcohol increased. Standard errors for estimated kinetic constants from a fit with HYPER were less than 15%. Concn represents the range used, K_m is the apparent Michaelis constant, k_{max} is the maximum rate constant for the transient oxidation, and ^Dk denotes the ratio of k_{max} for protio substrate to that of deuterio substrate.

isoabsorptive point for free and enzyme-bound forms of NADH (Theorell & Bonnichsen, 1951), was monitored for the oxidation of alcohols and the reduction of aldehydes. Maximum values for apparent rate constants for the oxidation and dissociation of alcohol and the reduction of aldehyde were obtained by fitting the observed rate constants to the expression $k_{obs} = k_{max}[S]/(K_m + [S])$ by using the HYPER program of Cleland (1979). The program NONLIN (C. M. Metzler, The Upjohn Co., Kalamazoo, MI) was used for general nonlinear regression analysis. Values for microscopic rate constants were estimated by progress curve analysis using the manual kinetic simulation program KINSIM (Barshop et al., 1983) and the automatic fitting routine FITSIM (Zimmerle et al., 1987).

Results and Discussion

Oxidation of Alcohols. The rate of interconversion of ternary complexes can be limited by the transfer of hydride ion from alcohol to NAD^+, the release of a proton to solvent, or other unimolecular steps. In order to probe for the rate-limiting step(s), the apparent first-order rate constants for the transient (pre-steady-state) oxidation of a series of alcohols were determined with varied concentrations of alcohols. The data fit Michaelis–Menten kinetics, and Table I summarizes the kinetic constants and observed primary isotope effects. The enzyme is more reactive (k/K_m) on longer chain alcohols, as is well-known from steady-state kinetics (Sund & Theorell, 1963; Pietruszko et al., 1973). A maximum rate constant of 180 s^{-1} for the oxidation of ethanol agrees well with the value previously reported (Brooks & Shore, 1971; Brooks et al., 1972). This rate constant increased to 310 s^{-1} for 1-propanol but was not much faster with 1-butanol and 1-hexanol.

As the chain length of alcohol increased, the observed kinetic isotope effect decreased, consistent with an increased commitment to catalysis. An isotope effect, ^Dk, of 3.8 was observed for the transient oxidation of ethanol-d_5, but this is a combination of primary and secondary isotope effects. Corrected for the contribution from secondary isotope effects, the observed primary isotope effect is about 2.6. The observed substrate isotope effect for 1-butanol was only 1.3. When the reactions of propanol or butanol with enzyme–NAD^+ complex (preformed in one syringe) were measured, the maximum rate constant was 440 s^{-1}, and the isotope effect was 2. The small isotope effects could be due either to a small intrinsic isotope effect or to a rate-limiting step prior to hydride transfer. The latter is more likely because the intrinsic isotope effects determined for the oxidation of alcohols by NAD^+ are between 4 and 8 (Cook & Cleland, 1981b,c; Damgaard, 1981; Scharschmidt et al., 1984). Thus, the results suggest that isomerization of the E–NAD^+ complex, which occurs at 620 s^{-1} at pH 8 (Sekhar & Plapp, 1988), is partially, but not fully, rate-limiting for the oxidation of longer chain alcohols.

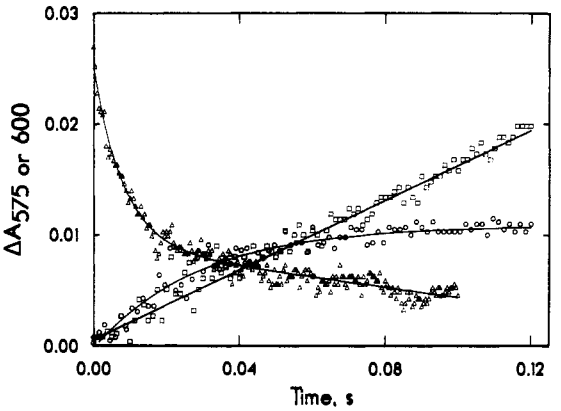

FIGURE 1: Proton release and uptake in transient reactions. Oxidation of 7.5 mM 1-propanol by 2 mM NAD^+ in the presence of 20 μN enzyme and 30 μM chlorophenol red at pH 5.9 (A_{575}, △). Proton uptake during the reduction of 0.5 mM acetaldehyde by 0.1 mM NADH with 20 μN enzyme under turnover conditions (A_{600}, □), and during the reduction of 20 mM acetaldehyde in the presence of 10 mM pyrazole by 0.1 mM NADH (A_{600}, ○), at pH 9 in the presence of 25 μM thymol blue. The curves are fits to functions for a single exponential followed by a zero-order steady state (△), a line (□), and a single exponential (○).

Table II: Apparent Rate Constants for Proton Release or Uptake[a]

substrate	concn (mM)	pH	k_{obs} (s^{-1})	k_{328} (s^{-1})
1-propanol	7.5	5.9	180	110
1-butanol	2.5	5.9	170	100
CF_3CH_2OH	8.0	7.6	>1000	
pyrazole	7.5	7.6	>1000	
ethanol	160	7.6	500	130
1-propanol	7.5	8.0	460	290
1-butanol	2.5	8.0	460	
1-propanol	25	9.0	450	210
acetaldehyde	20	9.0	44	270

[a] About 40–50 μN of enzyme with 10–30 μM indicator in a weak buffer of 1 mM sodium phosphate or 0.5 mM $Na_4P_2O_7/H_3PO_4$ and 33 mM Na_2SO_4 from one drive syringe was mixed with an equal volume of 4 mM NAD^+ and the stated concentrations of alcohol or pyrazole with the same concentration of indicator in the same buffer from the other syringe. Chlorophenol red (575 nm, 30 μM), phenol red (560 nm, 10 μM), and thymol blue (600 nm, 20 μM) were the indicators used for measurements at pH 5.9, 7.6 and 8.0, and 9.0, respectively. A biphasic disappearance of absorbance due to proton release was observed for the oxidation of alcohol, and the data were fitted to an equation for a single-exponential process followed by a zero-order steady state. Proton uptake at pH 9 during the reduction of 20 mM acetaldehyde, with 0.1 mM NADH and 10 mM pyrazole (Figure 1), was studied in the presence of 25 μM thymol blue. Acetaldehyde concentrations above 20 mM produced a superfluous release of protons. k_{obs} denotes the observed rate constant for proton release or uptake, and k_{328} represents the rate constant for transient oxidation of alcohol or reduction of acetaldehyde.

Proton Release from Enzyme-Bound Alcohol. Proton transfer in the mechanisms of dehydrogenases is usually treated as a rapid equilibrium process. Nevertheless, the rate may be comparable to other rates in the mechanism or be limited by other steps. Figure 1 shows that proton release during the oxidation of 1-propanol was biphasic with a burst phase followed by a steady-state release of protons. Table II lists the apparent rate constants for proton release for different substrates or inhibitors. Proton release, k_{obs}, is faster than coenzyme reduction, k_{328}, over a wide range of pH, suggesting that proton release from enzyme-bound alcohol precedes the

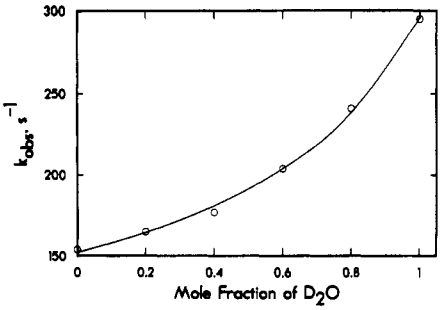

FIGURE 2: Proton inventory for the transient oxidation of ethanol. Buffers at pL 8.0 and 25 °C containing different mole ratios of D_2O were prepared as described by Schowen and Schowen (1982). Rate constants for at least duplicate reactions of 10 μN enzyme, 2 mM NAD^+, and 50 mM ethanol are plotted as points, and the curve results from the fit with NONLIN to the equation: $k_n = k_0(1 - n + n\phi_T)/(1 - n + n\phi_R)$, where n is the mole fraction of D_2O in the reaction medium and the fitted parameters were 152 s^{-1} for k_0, 0.37 for the fractionation factor in the reactant state (ϕ_R), and 0.73 for the transition state (ϕ_T).

Scheme I

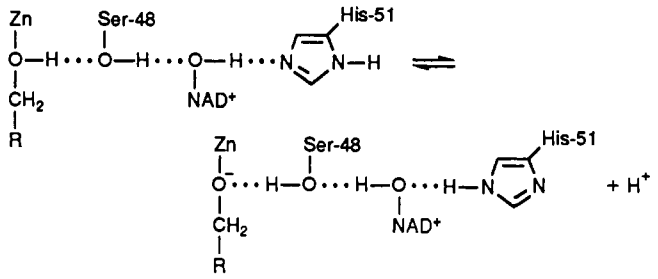

transfer of hydride ion from alcohol to NAD^+. With ethanol, 1-propanol, and 1-butanol a limiting value of 500 s^{-1} was seen at pH 7.6 and higher. However, rates measured with pyrazole and trifluoroethanol suggest that proton release is very fast. When 2,2,2-trifluoroethanol or pyrazole were used instead of a substrate, the rate of proton release from the ternary complex seemed to be limited by a preceding step in the mechanism, the isomerization of the enzyme–NAD^+ complex, with an estimated rate constant of about 1100 s^{-1} at pH 7.6 (Sekhar & Plapp, 1988).

A rapid proton release is expected because of base catalysis by His-51 acting through the proton relay system (Scheme I; Eklund et al., 1982). Chemical modification of histidines in the liver enzyme (Hennecke & Plapp, 1983) and site-specific replacement of His-51 by glutamine in the yeast enzyme (Gould, 1988) support such a mechanism. It appears that neither binary complex isomerization nor loss of a proton from enzyme-bound alcohol is completely rate-limiting, but both of them partially limit the rate of hydride transfer, which results in small observed isotope effects on transient oxidation of longer chain alcohols.

Solvent Isotope Effect and Transition-State Structure. A proton inventory for the pre-steady-state oxidation of ethanol was determined by studying the kinetics at saturating concentrations of NAD^+ and ethanol (Figure 2). The rate of reaction was faster in D_2O, and an inverse solvent isotope effect of 2.0 was observed. The data were fitted most simply by the Gross–Butler equation with one protonic site having different fractionation factors in reactant and transition states.

The data suggest that the reactant state is enzyme-bound alkoxide. A ϕ of about 0.5 is suggested for a protonic site hydrogen bonded with hydroxide or alkoxide ion in aqueous medium (Schowen & Schowen, 1982), but in the gas phase or nonaqueous solvents fractionation factors are lower, and in acetonitrile a value of 0.31 has been measured by Kreevoy and Liang (1980). Water is excluded from the active site in the enzyme–substrate complex; hence, a ϕ value of 0.37 is reasonable. As shown above (Scheme I), the hydroxyl group of Ser-48 forms a hydrogen bond with the oxygen of the alcoholate and can be responsible for the observed solvent isotope effect. The other protonic sites in the hydrogen-bonded system have fractionation factors of unity (Schowen & Schowen, 1982). A ϕ of 0.73 for the protonic site in the transition state suggests that the charge on the alkoxide in this state is −0.3 ($0.37^{0.31} = 0.73$). This implies that the transition state is not symmetric, but more like aldehyde, with the hydride ion closer to C-4 of the nicotinamide than to alcoholate.

Table III: Kinetic Constants for the Transient Reduction of Aldehydes and Cyclohexanone[a]

substrate	concn (mM)	K_m (mM)	k_{max} (s^{-1})	k_{off} (s^{-1})	k/K_m (mM^{-1} s^{-1})
acetaldehyde	0.1–10	2.1	390	240	185
acetaldehyde[b]	0.1–10	5.8	350	220	61
propanal	0.1–10	0.49	410	110	850
propanal[b]	0.1–10	0.60	480	100	710
butanal	0.02–1.0	0.05	490	81	9700
butanal[b]	0.025–1.0	0.06	550	80	8700
hexanal	0.02–1.0	0.04	520	74	14000
benzaldehyde	0.025–2.5	0.49	320	52	660
benzaldehyde[b]	0.025–2.5	0.70	170	56	250
cyclohexanone	10–225	38	84	fast[c]	2.2
cyclohexanone[b]	10–225	38	35	fast[c]	0.91

[a] Enzyme (about 10 μN) reacted with 0.1 mM NADH or NADD and the varied concentration of aldehyde and 20 mM pyrazole, which limited the reaction to a single turnover (McFarland & Bernhard, 1972). At low concentrations of aldehyde, the reaction was described by a single-exponential function, but when concentrations of aldehyde were saturating, fits to a double-exponential function were better. In some cases, inhibition at high concentrations of aldehyde was observed; these data were excluded. During the reduction of butanal, the biphasic nature of the reaction (fast phase followed by a slow phase) was evident even at low concentrations. The first-order rate constants (for the faster phase, when biphasicity was observed) were fitted with HYPER to obtain the maximal rate constants (k_{max}) and Michaelis constants (K_m). Apparent rate constants for the desorption of alcohol (k_{off}) from the ternary complexes (E–NAD^+–alcohol) were measured by following the formation of E–NAD^+–pyrazole complex at 300 nm (ϵ = 7.2 mM^{-1} cm^{-1}), which is concomitant with dissociation of alcohol and occurs after the reduction of aldehyde by NADH. Standard errors in the estimation of kinetic constants were 15% or better. [b] NADD was used. [c] The rate of formation of E–NAD^+–pyrazole was the same as that of transient reduction of cyclohexanone, and hence the desorption of cyclohexanol was assumed to be rapid.

The transition state suggested for the oxidation of ethanol might be different with other substrates. Theoretical calculations suggest that the reaction of formaldehyde with an NADH analogue has a symmetric transition state, with the charge on alkoxide being −0.5 (Tapia et al., 1988). The transient rate of oxidation of benzyl alcohol has an inverse 1.3-fold solvent isotope effect (Schmidt et al., 1979), not 2-fold as we found with ethanol.

The reduction of an aldehyde should show a normal solvent isotope effect with the proposed transition state. The rate of benzaldehyde reduction by NADH in D_2O was decreased as expected, but only by 15% at the most. This change was too small to attempt a proton inventory. Similar observations were reported earlier for the reduction of naphthaldehyde by Schmidt et al. (1979). In contrast, Welsh et al. (1980) found an inverse isotope effect of 1.5–2.0 for the reduction of *p*-methoxybenzaldehyde catalyzed by yeast alcohol dehydrogenase. The significant kinetic steps in the reduction of benzaldehyde by the yeast enzyme appear to be different from those of liver enzyme.

Reduction of Aldehydes. The kinetics of transient reduction (single turnover) showed saturation behavior (Table III). The maximum rate constant for acetaldehyde reduction was sig-

nificantly faster than the value of 90 s^{-1} previously reported (Kvassman & Pettersson, 1976). We could reproduce the results of other workers (Jacobs et al., 1974; Kvassman & Pettersson, 1976) with benzaldehyde as a substrate. A smaller value of K_m and a larger k/K_m with increased chain length of aldehyde parallel similar observations with alcohols. However, it was surprising that the apparent maximum rate constant for the transient reduction of aldehyde did not change significantly with the substrate and that there was practically no substrate isotope effect. In contrast, substrate isotope effects of 1.9 and 2.4 were observed with benzaldehyde and cyclohexanone, respectively.

The intrinsic isotope effects for the reduction of aliphatic aldehydes by the horse enzyme have not been directly determined. However, Cook et al. (1980) determined that the isotope effect on the equilibrium constant ($^DK_{eq}$) for the reaction of ethanol with NAD^+ is 1.07. If the intrinsic kinetic isotope effect for the oxidation of ethanol is 8 (Damgaard, 1981), the calculated intrinsic isotope effect for the reduction of aldehyde would be 7.4. Thus, the lack of isotope effect on the rate of reduction of aldehydes is not due to a negligible intrinsic effect but stems from a rate-limiting step prior to hydride transfer. With 3-acetylpyridine adenine dinucleotide (an analogue with a more positive redox potential than NAD^+), a kinetic isotope effect of 3.3 was observed by us for the reduction of acetaldehyde, supporting the argument that the intrinsic isotope effect for the reduction of aldehyde is sizable. Furthermore, the turnover numbers for the reduction of acetaldehyde with enzymes imidylated at Lys-228 are 800–1100 s^{-1} (Zoltobrocki et al., 1974; Plapp et al., 1986). This modification places a bulky group in the active site, resulting in weaker binding and faster dissociation of coenzyme. The rate-limiting step is changed from coenzyme dissociation to hydride transfer. Thus, the rate constant for reduction of acetaldehyde by native enzyme could be faster than the observed rate constant of 400 s^{-1}, and the data imply that there is a rate-limiting step(s) prior to reduction of aldehyde.

Binding of NADH. If the rate constant for a conformational change that occurs when NADH binds to enzyme is slower than that of hydride transfer from NADH to aldehyde, a limiting rate for the reduction of aldehydes and no substrate isotope effect would be observed. The dependence of observed rate constant for NADH binding on the concentration of NADH (Figure 3) showed no evidence of saturation in the concentration range studied, suggesting that the rate of conformational change is faster than 1000 s^{-1} and not within the range of measurement of our stopped-flow apparatus. The slope of the line in Figure 3 represents the bimolecular rate constant for the binding of coenzyme, 1.0×10^7 M^{-1} s^{-1}, which agrees with the rate constant measured by others (Plapp et al., 1973; Kvassman & Pettersson, 1979).

These studies (Figure 3) and others (Geraci & Gibson, 1967) suggest that isomerization of E–NADH is relatively fast. Kinetics of acetaldehyde reduction by preformed E–NADH complex showed an increase in limiting rate constant to 600 s^{-1}, suggesting that isomerization of enzyme–NADH complex could be partially rate-limiting. However, when NADD was used (in the E–NADD complex), no isotope effect was observed on reduction of acetaldehyde. Therefore, the rate-limiting step must be at the ternary complex level. From the proton uptake studies, it is evident that the aldehyde is not protonated prior to hydride transfer. The rate constant for proton uptake is an order of magnitude slower than that of hydride transfer and corresponds to the rate of dissociation

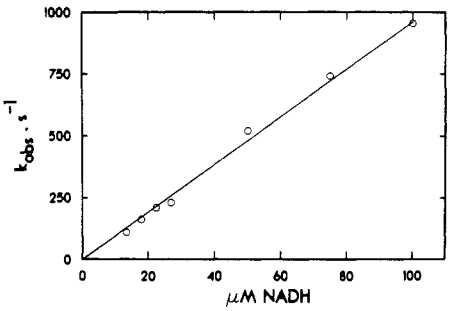

FIGURE 3: Dependence on concentration of binding of NADH. Enzyme was mixed with NADH, and the reaction was monitered by the decrease in absorbance (10 μN enzyme and 50–100 μM NADH) due to the shift in the spectrum of NADH at 355 nm in the stopped-flow spectrophotometer or by protein fluorescence quenching (2 μN enzyme and 13–27 μM NADH, λ_{ex} = 285 nm and λ_{em} = >315 nm) in a Durrum-Gibson stopped-flow spectrofluorometer. Points are average values from two to four reactions fitted to an equation for a first-order process, and the line is fitted by NONLIN.

of alcohol. Thus the rate-limiting step prior to hydride transfer is probably an isomerization of the E–NADH–aldehyde complex. Such an isomerization has been invoked to explain the kinetic isotope effects for the reactions catalyzed by yeast alcohol dehydrogenase (Cook & Cleland, 1981a).

Dissociation of Alcohols from Ternary Complex. The rate of dissociation of alcohol from the E–NAD^+–alcohol complex was measured by trapping the E–NAD^+ complex with saturating concentrations of pyrazole (Table III). The rate of formation of E–NAD^+–pyrazole corresponds to the rate of desorption of alcohol, provided that the rate of hydride transfer is significantly faster than the release of alcohol. This is probably true for longer chain aldehydes and aromatic aldehydes such as benzaldehyde. For acetaldehyde, however, the rates of hydride transfer and alcohol release could be comparable, and the formation of E–NAD^+–pyrazole represents the lower limit for release of ethanol.

As might be anticipated, the apparent rate constant for the desorption of alcohols gradually decreases as the chain length is increased. Aromatic substrates and long-chain aliphatic substrates should make favorable contacts with hydrophobic amino acid residues in the active site and be more tightly bound (Sund & Theorell, 1963). For secondary alcohols, however, this rate constant seems to be fairly large (Lee et al., 1988). For example, with cyclohexanone, the rate of formation of E–NAD^+–pyrazole is the same as the rate of reduction, suggesting that the release of cyclohexanol is very fast.

The pH dependence for dissociation of 1-butanol (Figure 4) indicates that this rate is maximal below a pK of 7.2. Apparently, the enzyme-bound alcohol must be protonated in order to dissociate rapidly, and a functional group or system with a macroscopic pK of 7.2 governs this process. The microscopic origin of this pK is probably either His-51 or the enzyme-bound alcohol itself, which are connected by the hydrogen-bonded system (Scheme I). A functional group that deprotonates with a pK between 6 and 7 to increase the rate of oxidation of alcohols has been reported for several substrates and has been assigned to this hydrogen-bonded system (Brooks et al., 1972; Kvassman & Pettersson, 1978; Pettersson, 1987; Sekhar & Plapp, 1988). A pK of 7.2 observed for dissociation of 1-butanol agrees well with the pK of this macroscopic system.

Simulations and Estimation of Rate Constants. Steady-state kinetics, product and dead-end inhibition studies, and isotope exchange at equilibrium show that the simplest mechanism that describes the action of the horse enzyme is predominantly Ordered Bi Bi with the probable isomerization

Table IV: Estimated Rate Constants for Alcohol Oxidation and Aldehyde Reduction[a]

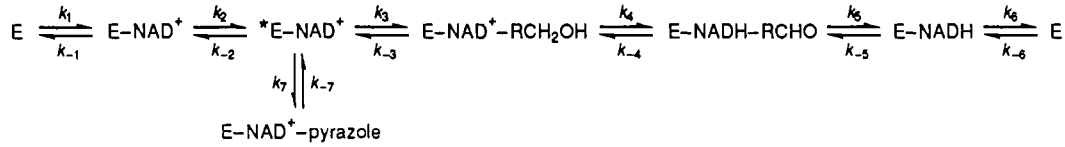

rate constant	substrate			
	ethanol	1-propanol	1-butanol	benzyl alcohol
k_3 (M^{-1} s^{-1})	2.4×10^5	1.2×10^6	9.7×10^5	3.7×10^6
k_{-3} (s^{-1})	560	410	84	58
k_4 (s^{-1})	490 (150)[b]	380 (280)	380 (390)	38 (6.2)
k_{-4} (s^{-1})	610 (360)	600 (550)	600 (820)	310 (110)
k_5 (s^{-1})	64	39	17	66
k_{-5} (M^{-1} s^{-1})	9.2×10^4	1.3×10^6	2.8×10^6	8.3×10^5

[a] Rate constants for the binding of NADH and NAD^+ (purified on a DEAE-Sepharose column) and pyrazole were estimated by the progress curve analysis [as in Sekhar and Plapp (1988)] and were fixed in all simulations: k_1 (4.5×10^7 M^{-1} s^{-1}), k_{-1} (2.3×10^4 s^{-1}), k_2 (620 s^{-1}), k_{-2} (64 s^{-1}), k_6 (5.5 s^{-1}), k_{-6} (1.1×10^7 M^{-1} s^{-1}), k_7 (1.2×10^5 M^{-1} s^{-1}), and k_{-7} (0.01 s^{-1}). Eight progress curves, four forward and four reverse reactions, from the experiments described in Tables I and III were used for these simulations. Some of the rate constants for the oxidation of 1-propanol and reduction of propanal are different from those reported previously, where only reactions in the forward direction were analyzed (Sekhar & Plapp, 1988). Standard errors in the estimation of the rate constants were 10% or better. [b] Values given in parentheses are for deuterio substrates; for these substrates all rate constants as obtained for protio substrates were fixed except the isotope-sensitive ones, k_4 and k_{-4}.

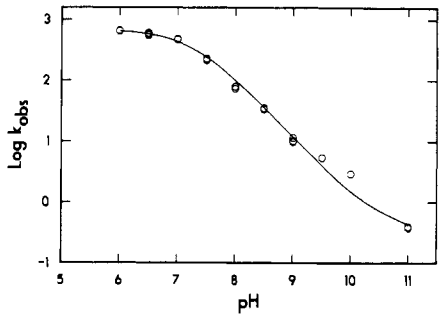

FIGURE 4: pH dependency for dissociation of 1-butanol from the E–NAD^+–alcohol complex. The rate constants were measured after mixing 20 μN enzyme and 0.2 mM NADH in a weak buffer with saturating concentrations of butanal (20 mM) and pyrazole (20 mM) in double strength buffers of the desired pH. These were 20 mM $Na_4P_2O_7$ adjusted to the desired pH with H_3PO_4 and to a final ionic strength of 0.2 with sodium phosphate buffer for pH 5.5–9.0, and 66 mM Na_2HPO_4 adjusted with glycine above pH 9. The increase in absorbance due to E–NAD^+–pyrazole was fit by a single exponential. NONLIN was used to fit the pH dependence with the equation: $k_{obs} = \{k_{max} + (k_{min}K_a/[H^+])\}/(1 + K_a/[H^+])$. Values of 630 s^{-1} for k_{max}, 0.4 s^{-1} for k_{min}, and 7.2 for pK_a were obtained.

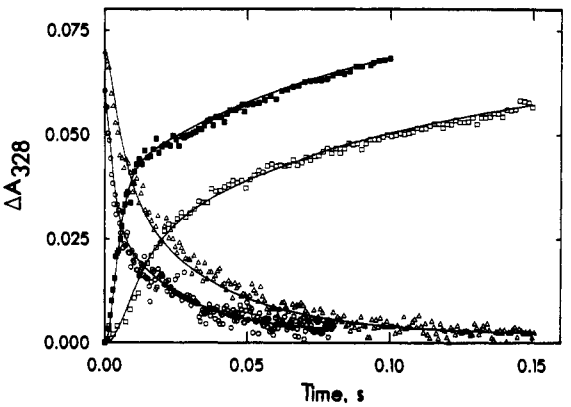

FIGURE 5: Progress curves simulated for the mechanism in Table IV for the transient oxidation of 1-butanol and the reduction of butanal (pseudo single turnover) at pH 8 and 25 °C. Enzyme (10 μN) reacted with 2 mM NAD^+ and 0.1 mM (□) or 0.75 mM (■) butanol; enzyme (7 μN) reacted with 0.1 mM NADH and 50 μM (△) or 0.25 mM (○) butanal in the presence of 20 mM pyrazole.

of the enzyme–NAD^+ complex (Wratten & Cleland, 1963; Dworschack & Plapp, 1977; Silverstein & Boyer, 1964; Plapp et al., 1986). Structural studies (Eklund et al., 1981; Eklund & Brändén, 1987), relaxation studies (Coates et al., 1977; Hardman, 1981), and transient kinetics (Sekhar & Plapp, 1988) confirm that the binding of NAD^+ to the enzyme is a two-step process and show that a rapid association is followed by an isomerization of the E–NAD^+ complex. To assign values for all the rate constants in the mechanism, we analyzed the progress curves. Initial estimates were obtained by manual simulations of each curve with KINSIM, and then all curves were simultaneously fitted with FITSIM. Figure 5 shows that the data agreed reasonably well with the progress curves simulated for the mechanism and constants in Table IV.

The rate constants estimated from simulations (Table IV) were used to calculate kinetic constants, such as K_a, K_{ia}, K_b, K_p, K_q, V_1, V_2, and K_{eq}, by using the equations from Plapp (1973). These calculated values agreed very well with those determined by steady-state kinetics (Dworschack & Plapp, 1977), indicating that the estimated rate constants are consistent with the experimental observations.

However, the mechanism in Table IV does not account for the observation (Table I) that oxidation of alcohols of increasing chain length approached a limiting rate and had a decreasing substrate isotope effect. As discussed previously, the isomerization of the E–NAD^+ complex precedes and partially limits the rate of oxidation of alcohols. Loss of the proton from alcohol and its release to solvent may also be kinetically significant, controlling the rate of a subsequent hydride-transfer step. Thus, we incorporated the release of proton from alcohol into the mechanism and attempted to estimate the rate constants (Table V). This simulation was improved by constraining the ratio of k_4 to k_{-4} to fit a pK value of 7.2. Nevertheless, standard errors for some of the rate constants were large, indicating that a range of values could describe the data. The rate constant for the loss of the proton may be as fast as 10^4 s^{-1}, but the observed rate constant will be less than 620 s^{-1} due to a limiting rate of isomerization of the E–NAD^+ complex.

The rate constants in Table V were used to simulate the progress curves for oxidation of alcohols, reduction of aldehydes, release of a proton, and release of alcohols from ternary complexes. The apparent first-order rate constants for the simulated curves agreed well with the rate constants observed (Table VI). These simulations also showed the following. (1) The observed rate of proton release is not very sensitive to changes in the input rate constants. The actual rate constant for proton release (k_5) could be restricted to 500 s^{-1} by the

Table V: Estimated Rate Constants for the Mechanism with an Alkoxide Intermediate[a]

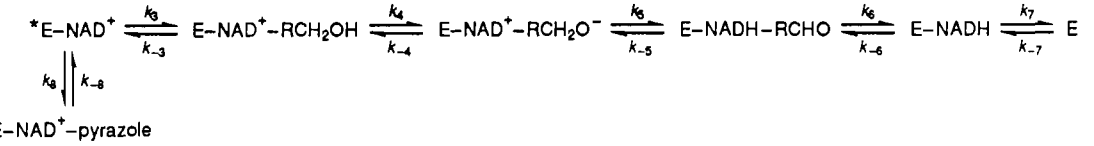

rate constant	substrate			
	ethanol	1-propanol	1-butanol	benzyl alcohol
k_3 (M^{-1} s^{-1})	3.2×10^5*	2.1×10^6*	1.0×10^6	2.0×10^6
k_{-3} (s^{-1})	4900*	4800*	600	160
k_4 (s^{-1})	8000*	5800*	7300	3600*
k_{-4} (s^{-1})[b]	1300*	960*	1200	560*
k_5 (s^{-1})	520	490	450	23
k_{-5} (s^{-1})	530	680	620	240
k_6 (s^{-1})	61	43	17	170
k_{-6} (M^{-1} s^{-1})	2.2×10^5	2.0×10^6	2.9×10^6	3.2×10^6

[a] Rate constants for steps 1, 2, 7, and 8 were fixed with the values given in Table IV. The ratio of k_4 to k_{-4} was maintained at 6 so that the pK value for the ionization of E-NAD$^+$-alcohol is 7.2. Standard errors for the estimated rate constants were 10% or better, except for those marked with an asterisk, for which the error limits ranged from 30 to 50%. If the ratio of k_4 to k_{-4} was not fixed, standard errors for several rate constants were larger than 50%, and the calculated pK for step 4 ranged from 7.3 to 8.3. [b] This is the apparent first-order rate constant at pH 8; multiply by 10^8 M^{-1} for the second-order rate constant.

Table VI: Comparison of Calculated and Observed Kinetic Constants for Reactions of Ethanol and Acetaldehyde[a]

kinetic constant	calculated	determined
k_{oxidn} (s^{-1})	210	180
k_{oxidn}, ethanol-d_5 (s^{-1})	41	47
k_{off}, ethanol[b] (s^{-1})	200	240
k_{H^+}[c] (s^{-1})	610	500[d]
k_{redn} (s^{-1})	400	390
k_{redn}, NADD (s^{-1})	75	360
K_{eq}[e] (pM)	10	10[f]

[a] Progress curves were simulated by using the rate constants given in Table V and the NONLIN program was used to compute kinetic constants. k_{oxidn} and k_{redn} represent the apparent rate constants for transient oxidation of ethanol and reduction of acetaldehyde, respectively. An intrinsic isotope effect of 6 was used to calculate kinetic constants with deuterio substrates. [b] Apparent rate constant for the dissociation of ethanol from the enzyme-NAD$^+$-ethanol complex. [c] Rate constant for proton release from the E-NAD$^+$-ethanol complex. [d] Measured at pH 7.6. [e] Equilibrium constant for the reaction of NAD$^+$ with ethanol. [f] Sund and Theorell (1963).

Table VII: Estimated Rate Constants for the Reactions of Ethanol and Acetaldehyde[a]

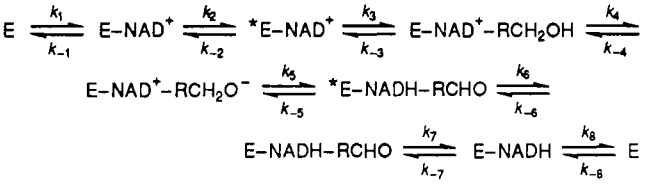

step	forward (k_n)	reverse (k_{-n})
1	4.5×10^7 M^{-1} s^{-1}	2.3×10^4 s^{-1}
2	620 s^{-1}	64 s^{-1}
3	3.2×10^5 M^{-1} s^{-1}	3600 s^{-1}
4	1.6×10^4 s^{-1}	2600 s^{-1}
5	780 s^{-1}	3100 s^{-1}
6	5500 s^{-1}	1500 s^{-1}
7	45 s^{-1}	2.3×10^5 M^{-1} s^{-1}
8	5.5 s^{-1}	1.1×10^7 M^{-1} s^{-1}

[a] Rate constants for steps 1, 2, 4, and 8 were fixed in the simulations. As the number of variables in this scheme is more than the number of input progress curves, FITSIM did not yield estimations with reasonable standard errors. Hence, manual variation with the program KINSIM was used to estimate these rate constants. The ratio of k_4 to k_{-4} was fixed at 6, so that the pK of the enzyme-NAD$^+$-alcohol complex is 7.2.

preceding rate constant of 620 s^{-1} for the isomerization of the enzyme-NAD$^+$ complex. (2) When a substrate isotope effect of 6 was introduced in the simulations, the observed rate constant for the oxidation of ethanol agreed well with the one calculated from the simulated progress curve, but the rate constant for the overall reduction of acetaldehyde by NADD was 4 times larger than the corresponding rate constant calculated from the simulated data (Table VI). Therefore, the mechanism in Table V does not explain the lack of isotope effect on the reduction of aldehydes.

An intrinsic primary isotope effect would not be observed on the rate of hydride transfer from reduced coenzyme to aldehyde if one of the preceding steps were rate-limiting. As described earlier, binding of NADH is not saturable up to 1000 s^{-1}, and hence the isomerization of E-NADH does not significantly limit the rate of hydride transfer. However, an isomerization of the enzyme-NADH-aldehyde complex (e.g., a rearrangement around the catalytic zinc) is first-order and could limit the rate of reduction of aldehyde. Thus, another step was added to the mechanism, and manual simulations were performed to produce a reasonable set of rate constants (Table VII). These rate constants for ethanol oxidation and acetaldehyde reduction are consistent with all of the experimental observations, including the dissociations of ethanol and a proton from the E-NAD$^+$-ethanol complex. Despite the overall consistency, the magnitudes of several of the rate constants remain provisional until confirmed by direct measurements of the rates of individual steps. Furthermore, there may be additional intermediates, or isomerizations, that have not been detected. Additional experiments are required to define the structures of the intermediates identified here by kinetic studies. The results provide a minimal mechanism for liver alcohol dehydrogenase.

ACKNOWLEDGMENTS

We thank Drs. C. T. Zimmerle and C. Frieden for providing the KINSIM/FITSIM programs. The Protein Structure Facility of The University of Iowa made the stopped-flow instruments available.

REFERENCES

Barshop, B. A., Wrenn, R. F., & Frieden, C. (1983) *Anal. Biochem. 130*, 134-145.

Brooks, R. L., & Shore, J. D. (1971) *Biochemistry 10*, 3855-3858.

Brooks, R. L., Shore, J. D., & Gutfreund, H. (1972) *J. Biol. Chem. 247*, 2382–2383.
Cleland, W. W. (1979) *Methods Enzymol. 63*, 103–138.
Coates, J. H., Hardman, M. J., Shore, J. D., & Gutfreund, H. (1977) *FEBS Lett. 84*, 25–28.
Colonna-Cesari, F., Perahia, D., Karplus, M., Eklund, H., Brändén, C.-I., & Tapia, O. (1986) *J. Biol. Chem. 261*, 15273–15280.
Cook, P. F., & Cleland, W. W. (1981a) *Biochemistry 20*, 1790–1796.
Cook, P. F., & Cleland, W. W. (1981b) *Biochemistry 20*, 1797–1805.
Cook, P. F., & Cleland, W. W. (1981c) *Biochemistry 20*, 1805–1816.
Cook, P. F., Blanchard, J. S., & Cleland, W. W. (1980) *Biochemistry 19*, 4853–4858.
Damgaard, S. E. (1981) *Biochemistry 20*, 5662–5669.
Dworschack, R. T., & Plapp, B. V. (1977) *Biochemistry 16*, 111–116.
Eklund, H., & Brändén, C.-I. (1987) *Active Sites of Enzymes* (Jurnak, F. A., & McPherson, A., Eds.) pp 73–142, Wiley, New York.
Eklund, H., Samama, J.-P., Wallén, L., Brändén, C.-I., Åkeson, Å., & Jones, T. A. (1981) *J. Mol. Biol. 146*, 561–587.
Eklund, H., Plapp, B. V., Samama, J.-P., & Brändén, C.-I. (1982) *J. Biol. Chem. 257*, 14349–14358.
Ganzhorn, A. J., & Plapp, B. V. (1988) *J. Biol. Chem. 263*, 5446–5454.
Geraci, G., & Gibson, Q. H. (1967) *J. Biol. Chem. 242*, 4275–4278.
Gould, R. M. (1988) Ph.D. Thesis, The University of Iowa, Iowa City, IA.
Hardman, M. J. (1981) *Biochem. J. Lett. 195*, 773–774.
Hennecke, M., & Plapp, B. V. (1983) *Biochemistry 22*, 3721–3728.
Jacobs, J. W., McFarland, J. T., Wainer, I., Jeanmaier, D., Ham, C., Hamm, K., Wnuk, M., & Lam, M. (1974) *Biochemistry 13*, 60–64.
Koerber, S. C., MacGibbon, A. K. H., Dietrich, H., Zeppezauer, M., & Dunn, M. F. (1983) *Biochemistry 22*, 3424–3431.
Kreevoy, M. M., & Liang, T. M. (1980) *J. Am. Chem. Soc. 102*, 3315–3322.
Kvassman, J., & Pettersson, G. (1976) *Eur. J. Biochem. 69*, 279–287.
Kvassman, J., & Pettersson, G. (1978) *Eur. J. Biochem. 87*, 417–427.
Kvassman, J., & Pettersson, G. (1979) *Eur. J. Biochem. 100*, 115–123.
Lee, K. M., Dahlhauser, K. F., & Plapp, B. V. (1988) *Biochemistry 27*, 3528–3532.
McFarland, J. T., & Bernhard, S. A. (1972) *Biochemistry 11*, 1486–1493.
Morris, R. G., Saliman, G., & Dunn, M. F. (1980) *Biochemistry 19*, 725–731.
Pettersson, G. (1987) *CRC Crit. Rev. Biochem. 21*, 349–389.
Pietruszko, R., Crawford, K., & Lester, D. (1973) *Arch. Biochem. Biophys. 159*, 50–60.
Plapp, B. V. (1973) *Arch. Biochem. Biophys. 156*, 112–114.
Plapp, B. V., Brooks, R. L., & Shore, J. D. (1973) *J. Biol. Chem. 248*, 3470–3475.
Plapp, B. V., Sogin, D. C., Dworschack, R. T., Bohlken, D. P., Woenckhaus, C., & Jeck, R. (1986) *Biochemistry 25*, 5396–5402.
Sartorius, C., Gerber, M., Zeppezauer, M., & Dunn, M. F. (1987) *Biochemistry 26*, 871–882.
Scharschmidt, M., Fisher, M. A., & Cleland, W. W. (1984) *Biochemistry 23*, 5471–5478.
Schmidt, J., Chen, J., DeTraglia, M., Minkel, D., & McFarland, J. T. (1979) *J. Am. Chem. Soc. 101*, 3634–3640.
Schowen, K. B., & Schowen, R. L. (1982) *Methods Enzymol. 87*, 551–606.
Sekhar, V. C., & Plapp, B. V. (1988) *Biochemistry 27*, 5082–5088.
Shore, J. D., Gutfreund, H., Brooks, R. L., Santiago, D., & Santiago, P. (1974) *Biochemistry 13*, 4185–4190.
Silverstein, E., & Boyer, P. D. (1964) *J. Biol. Chem. 239*, 3908–3914.
Sund, H., & Theorell, H. (1963) *Enzymes, 2nd Ed. 7*, 25–83.
Tapia, O., Cardenas, R., Andres, J., & Colonna-Cesari, F. (1988) *J. Am. Chem. Soc. 110*, 4046–4047.
Theorell, H., & Bonnichsen, R. (1951) *Acta Chem. Scand. 5*, 1105–1126.
Theorell, H., & Yonetani, T. (1963) *Biochem. Z. 338*, 537–553.
Welsh, K. M., Creighton, D. J., & Klinman, J. P. (1980) *Biochemistry 19*, 2005–2016.
Wratten, C. C., & Cleland, W. W. (1963) *Biochemistry 2*, 935–941.
Zimmerle, C. T., Patane, K., & Frieden, C. (1987) *Biochemistry 26*, 6545–6552.
Zoltobrocki, M., Kim, J. C., & Plapp, B. V. (1974) *Biochemistry 13*, 899–903.